# Cytoplasmic Organization in Cerebellar Dendritic Spines

DENNIS M. D. LANDIS and THOMAS S. REESE
*Department of Neurology, Massachusetts General Hospital, Boston, Massachusetts 02114; and Laboratory of Neurobiology, National Institute of Neurological and Communicative Disorders and Stroke, Bethesda, Maryland 20205*

ABSTRACT Three sets of filamentous structures were found to be associated with synaptic junctions in slices of cerebellar tissue prepared by rapid-freezing and freeze-etch techniques. The electron-dense fuzz subjacent to postsynaptic membranes corresponds to a web of 4–6-nm-diam filaments that were clearly visualized in rapid-frozen, freeze-etched preparations. Purkinje cell dendritic spines are filled with a meshwork of 5–7-nm filaments that were found to contact the spine membrane everywhere except at the synaptic junction, and extend through the neck of the spine into the parent dendrite. In addition, 8–10-nm microfilaments, possibly actin, were seen to be associated with the postsynaptic web and to extend into the body and neck of the spine. The arrangements and attachments of the filamentous elements in the Purkinje cell dendritic spine may account for its shape.

Dendritic spines were found to be a consistent feature of many neurons as soon as impregnation techniques became reliable at the turn of the century (47, 48). With the advent of electron microscopic techniques, it could be shown that most spines participate in the formation of synaptic junctions (14, 16, 42). However, the function of synaptic spines in synaptic transmission is still not clear, despite a variety of hypotheses and spirited debates (8, 15, 46, 53).

In previous studies of membrane structure at synaptic junctions, we found that both presynaptic and postsynaptic membranes at the synaptic junction between parallel fibers and Purkinje cell spines have consistent patterns of intramembrane particle distribution (36, 37; see also reference 22). The presynaptic membrane is characterized by large particles associated with the cytoplasmic half of the fractured membrane; similar particles at other synapses are thought to represent voltage-dependent calcium channels (44). The postsynaptic membrane has an aggregate of particles that are associated with the extracellular half of the fractured membrane, are coextensive with the widened synaptic cleft, and occupy the same position as the electron-dense material seen in thin-sectioned preparations. Presumably, these particles represent proteins associated with the postsynaptic membrane, but the function of these proteins is not certain. At the vertebrate neuromuscular junction, aggregates of particles in comparable positions probably represent acetylcholine receptors (26, 30, 49).

We have used rapid freezing (27–29, 58, 59), cryofracture, and freeze-etching techniques to learn more about the details of synaptic structure. "Cryofracture" is used to denote the process of fracturing frozen tissue at low temperature to avoid distortion of intramembrane particles at the instant of fracture (17, 18, 35, 38, 52). The particles in membranes fractured by this method may break at several levels within the hydrophobic membrane interior (23, 30, 38). This paper describes the particles, visualized in a similar manner, at the postsynaptic aggregate on spine synapses.

Freeze-etching is accomplished by leaving the fractured tissue in the vacuum chamber of the freeze-fracture apparatus for several minutes prior to replication; during this time, water sublimates from the frozen surface, exposing the freeze-dried structures below (20, 30, 31). In previous studies, soluble components of the cytoplasm were usually extracted prior to freeze-etching (25) so that they did not collapse onto and obscure the filamentous components; we realized a similar end by etching away only a small amount of water (38, 51). With this "shallow etching" technique, the complicated meshwork of filamentous structures in postsynaptic cytoplasm of spines is exposed. Similar filaments can be identified in rapidly frozen tissue prepared for thin-section study by freeze-substitution fixation. This paper presents a description of these filamentous systems and their relationship to the postsynaptic specialization on the dendritic spine. The arrangement of these filaments in the spine may account for its

THE JOURNAL OF CELL BIOLOGY · VOLUME 97 October 1983 1169–1178

complex shape.

## MATERIALS AND METHODS

C57BL/6 mice aged 30–60 d were decapitated, the calvarium was rapidly removed, and a hemispherical slab 3 mm in diameter was sliced from the lateral cerebellum. The cerebellar slab was mounted on the stage of a rapid-freezing apparatus, and the surface of the slice was frozen by impact against a copper block cooled by liquid helium (27–29). The interval from decapitation to freezing was ~20–35 s.

Frozen tissue was mounted on the stage of a Balzers 301 freeze-fracture apparatus (Balzers, Hudson, NH) fitted with a liquid helium-cooled specimen stage, and fractured at a specimen holder temperature of 20–40°K in a vacuum of 2–4 × $10^{-8}$ torr. The swing of the microtome knife in the Balzers apparatus was usually parallel to the plane of the frozen tissue, and the fracture generated as the knife grazed the tissue was a shallow (<20 μm) gouge into the surface. The specimen holder was then warmed to 160–165°K in <10 min, held at that temperature for 10–30 min, and then replicated at 123°K with a platinum alloy in an electron beam gun (38).

Tissue was prepared for thin-sectioning by freeze-substitution fixation (58, 59). Frozen tissue was placed on the frozen surface of 5% osmium tetroxide in acetone covered by liquid nitrogen and then warmed to 188–190°K. The tissue was held in the melted acetone at the same temperature for 12–72 h, and finally allowed to warm to 273°K. Some specimens were treated with 1% tannic acid in acetone, and all were stained en bloc with uranyl acetate in methanol. The tissue was embedded in Araldite (Polysciences Inc., Warrington, PA).

We describe several different filamentous systems in terms of apparent diameter and periodicity in shadowed specimens. The diameters were differentiated by means of cross comparisons within each replica and therefore are not absolutely consistent between different replicas. Even within the same replica, different regions of the fractured tissue may have been exposed to different amounts of the metal shadow during rotary shadowing, so that identical structures in two different regions may appear to have slightly different diameters.

## RESULTS

In favorable preparations, the plane of fracture could be followed as it passed through the pia-arachnoid and the glia limitans at the surface of the cerebellar cortex on into the superficial molecular layer. In this region of cerebellar cortex, Purkinje cell dendrites and stellate cells are virtually the only postsynaptic processes present. Parallel fiber axons establish synaptic junctions with Purkinje cell spines and with the spines, dendritic shifts, and perikarya of stellate neurons. A much smaller population of stellate cell axons synapses on the shafts of Purkinje dendrites.

### *Spines on Purkinje Dendrites*

Purkinje cell spines could be readily recognized by their shape and origin from Purkinje cell dendrites (Fig. 1). The shapes of the spines and the particle aggregates associated with the synaptic junctions in general were similar to those described in previous studies (36), which depended on tissue fixed by perfusion with aldehydes. In the rapidly frozen tissue, however, we recognized some spines that gave rise to a smaller excrescence, usually in the body of the spine opposite its neck (Figs. 1 and 8). These excrescences did not appear to be a variation of the membrane blebs that are associated with aldehyde fixation (24) because the membrane of the excrescence had a normal complement of particles, distributed primarily on the cytoplasmic membrane half (Figs. 1 and 8), and because the structure of the cytoplasm in the neck of the excrescence was similar to that elsewhere in the spine (see below).

### *Membrane Structure at Synaptic Junctions with Parallel Fibers*

Aggregates of particles associated with the extracellular half of the dendritic membrane and co-extensive with the synaptic cleft are a consistent feature of parallel fiber synaptic junctions with Purkinje cell spines and with stellate cells. In rapidly frozen tissue, the particles constituting the aggregate were heterogeneous in shape and size (Figs. 3 and 4). Most were globular, although some were shard-like, and their minimum diameter in rotary-shadowed preparations ranged from 4–12 nm. The cytoplasmic half of the fractured membrane facing the synaptic cleft had two consistent features: large pits, presumably expanded by the etching but complementary to particles associated with the extracellular half of the membrane, and a distinct paucity of particles (Fig. 2). However, there were fewer large pits on the cytoplasmic half of the fractured postsynaptic membrane than there were particles in the aggregate on its extracellular half, so not all particles leave a large pit on the cytoplasmic membrane half.

Where the plane of fracture entered the spine membrane at a synaptic cleft, etching revealed fibrillar material bridging the cleft. Some particles on the extracellular half of the fractured membrane appeared to be continuous with the fibrillar material in the cleft while others were not. Also encountered in the synaptic cleft were some fibrillar elements that had no obvious continuity with particles on the extracellular membrane half.

The relationships of intramembrane particles to the adjacent cytoplasm were difficult to see at the postsynaptic specialization of parallel fiber synapses on spines. Because the depth of etching (estimated from the number of filaments that became exposed) was only 20–30 nm, we obtained views of the postsynaptic web in the cytoplasm only when the plane of fracture passed through the spine cytoplasm near a postsynaptic specialization (Fig. 4). The course of such a fracture would have to be very close to the spine membrane, and thus it was not surprising that most such fractures were propagated through this membrane.

Parallel fibers also form synapses with an excitatory action on stellate cell dendrites and perikarya, and these synapses appeared identical to those on Purkinje spines in both thin section and freeze-fracture. The synaptic junctions at these synapses are also flat, so that oblique planes of fracture through the synaptic junction showing the relationships between various levels of postsynaptic structures were frequent. Here it was apparent that filaments 4–6 nm in diameter contacted the postsynaptic membrane and that their distribution was co-extensive with the aggregate of particles on the extracellular membrane half which characterized the postsynaptic specialization (Fig. 5; for comparison, Fig. 6 illustrates a nonjunctional region). These short filaments constituted a mesh which extended ~20 nm into the postsynaptic cytoplasm thereby obscuring the true cytoplasmic surface of the plasma membrane at the widened synaptic cleft. This mesh corresponded in size and distribution to the electron-dense "fuzz" seen in thin-sectioned tissue. In the few instances where the postsynaptic mesh could be identified in cross-fractured dendritic spines, it was also co-extensive with the synaptic junction (Fig. 4).

### *Structure of the Cytoplasm in Purkinje Cell Spines*

Three distinct sets of filamentous elements could be distinguished on the basis of diameter, distribution, and periodicity in the etched cytoplasm of Purkinje cell dendritic spines. The first of these was the mesh of short, branching or crossing filaments, 4–6 nm in diameter, which extended ~20 nm into the spine cytoplasm from the true cytoplasmic surface of the

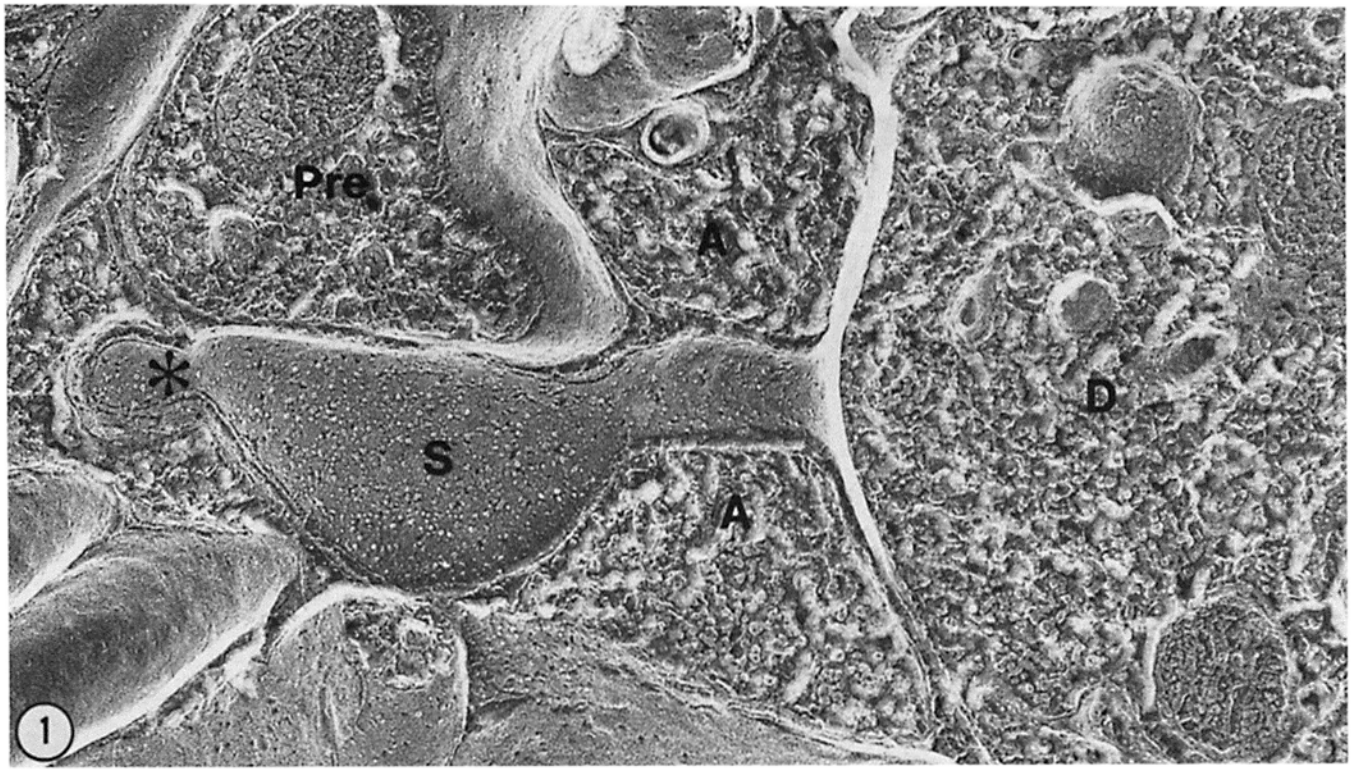



FIGURES 1 and 2 Fig. 1: Purkinje cell dendrite (*D*) and spine (*S*) contacted by a presynaptic varicosity (*Pre*) of a parallel fiber axon. The spine is otherwise ensheathed in astrocytic processes (*A*). These relationships correspond to those that have been established in thin section views, and make the identification of Purkinje cell spines obvious. This spine has a protuberance (asterisk) at the end opposite its neck. × 90,000. Fig. 2: Purkinje cell dendritic spine contacted by a cross-fractured parallel fiber axon. The parallel fiber axon, to the left of the illustration, has been cross-fractured near its synaptic junction with the Purkinje dendritic spine. The approximate location of the synaptic junction is revealed by an array of pits (arrows) on the cytoplasmic half of the freeze-fractured spine membrane. There is a large invagination in the plasmalemma of the parallel fiber axon and a protuberance (asterisk) on the dendritic spine at the upper right, both of which may be indicative of intense activity just before freezing. × 174,000.

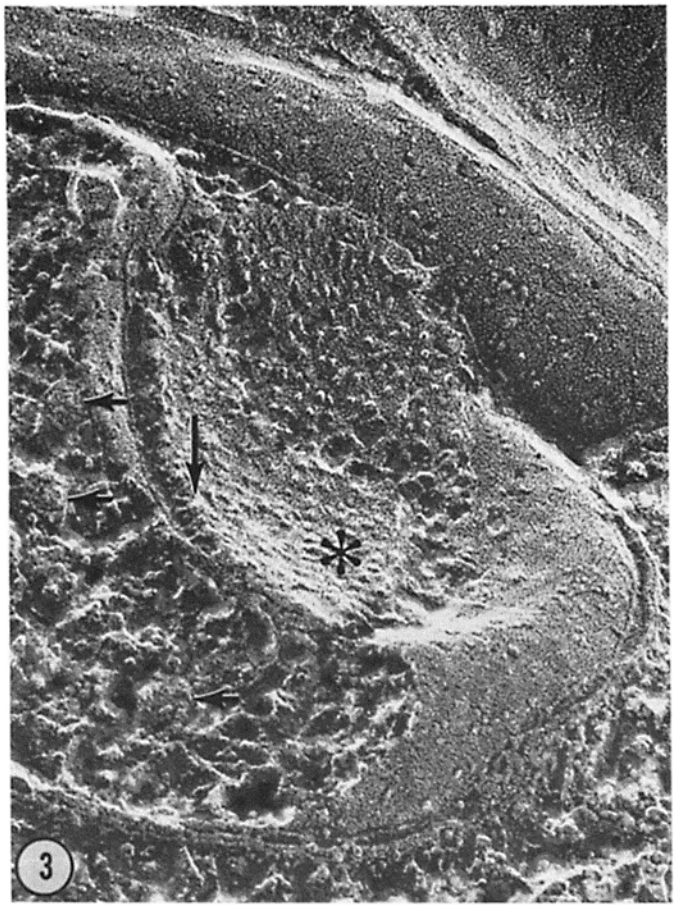

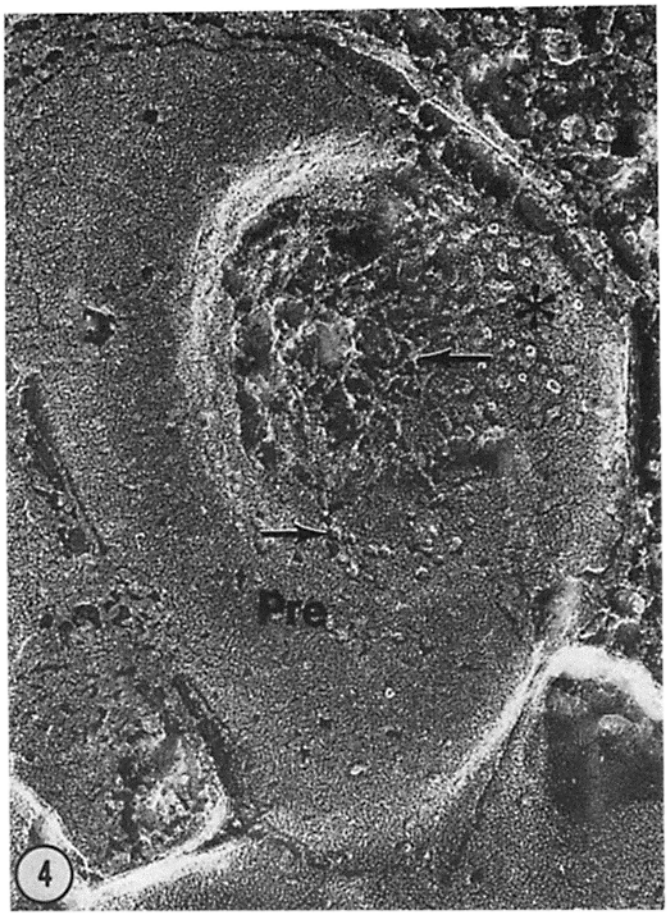
Pre

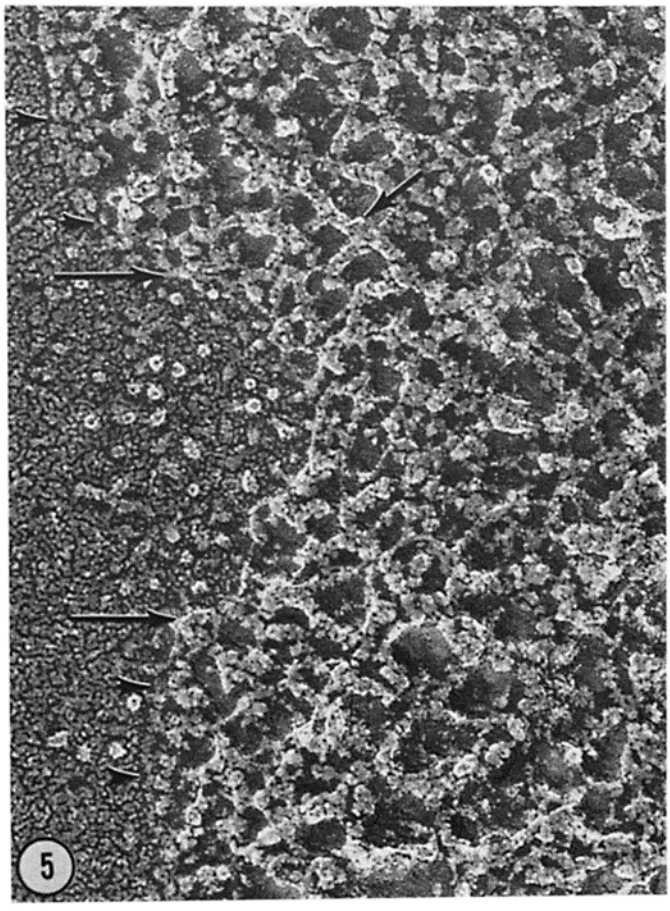

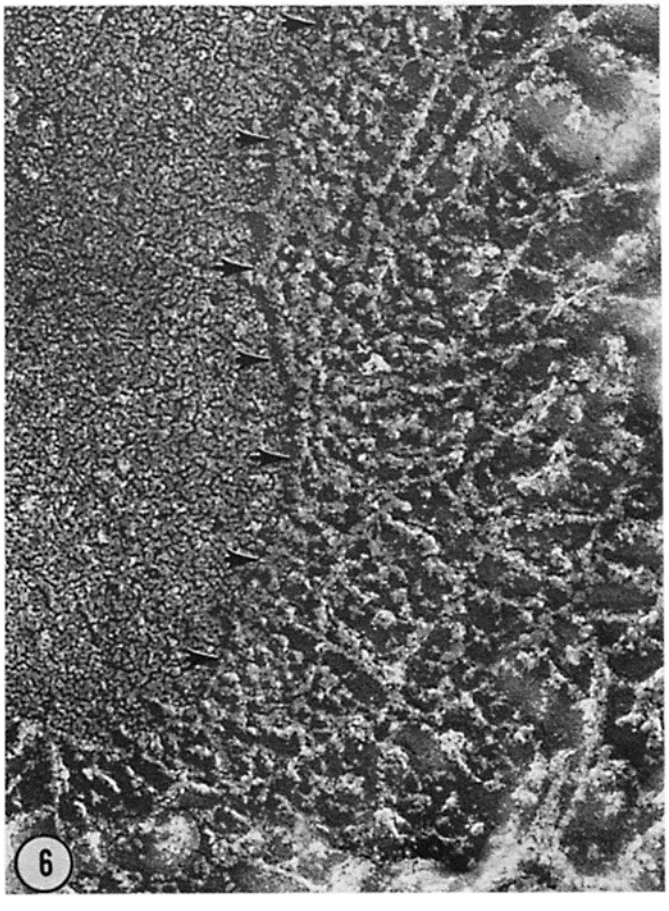

spine membrane at the synaptic cleft. As noted above, this mesh probably corresponded to the electron-dense fuzz of the postsynaptic specialization as visualized in thin-sectioned tissue (Fig. 11).

A second system of filamentous elements were 8–10 nm in diameter, frequently had a 4-nm periodicity, and were relatively straight. These microfilaments were most abundant in the body of the spine, were found consistently deep to the postsynaptic mesh, and extended through the neck of the spine into the parent dendrite (Figs. 7–10). They infrequently contacted the true cytoplasmic surface of the spine membrane, but lay in the vicinity of and sometimes contacted the 4–6-nm filaments in the postsynaptic mesh.

The third system of filaments was the most abundant (Figs. 7–10). These were 5–7 nm in diameter and were concentrated in a zone up to 40-nm wide next to the membrane. These filaments were fairly straight, crossed or branched at nodes, and often terminated in apposition to the true cytoplasmic surface of the spine membrane. They were often seen to intersect with the microfilaments, but did not seem to be continuous with them. The mesh formed by these filaments constituted the major filamentous element of the cytoplasm in the neck of the spine. These fine filaments were less densely packed in the core of the spine body where the microfilaments are relatively concentrated.

All three types of filaments were identified in the vicinity of parallel fiber synaptic junctions with stellate cells (Fig. 5). The short filaments obscuring the true cytoplasmic surface of the membrane at the synaptic cleft have already been described. Microfilaments were a constant feature of the cytoplasm deep to this mesh. Where etching exposed the true cytoplasmic surface of stellate cell processes and Purkinje cell dendrites outside of junctional regions, a few 5–7-nm filaments were found near the true cytoplasmic membrane surface (Fig. 6). This group of filaments resembled in every respect the fine filaments in the spine, but were more sparse. Microfilaments, identified by their larger diameter, occasionally coursed parallel to the true inner surfaces of nonjunctional dendritic membranes.

Granular material was interspersed within the filamentous meshworks in the spine and dendritic cytoplasm. The granules were irregular, often isolated, and ranged up to 20 nm in diameter. The numbers and shapes of these granular structures were similar in spines and dendrites (Figs. 7–9). It is these components that become aggregated and progressively obscure the filamentous elements unless the etching is carefully limited to removing 30 nm or less of water. It is probable that they represent soluble cytoplasmic components (51).

The Purkinje cell dendritic spines also contained membrane-limited cisterns (Figs. 7–9). When fractured, these membranes had a few particles associated with the luminal half of the membrane, and more particles associated with the half of the membrane adjacent to the spine cytoplasm (Figs. 7–9). The fine 5–7-nm filaments in the spine cytoplasm often coursed immediately adjacent to the cistern, but did not appear to insert into its membrane. Furthermore, we recognized no instances in which the microfilaments ended in apposition to a membrane cistern.

It was also possible to identify the various filamentous structures in Purkinje cell dendritic spines in thin sections of rapidly frozen tissue prepared by freeze-substitution fixation (Figs. 11 and 12). The filaments were electron-dense, tended to lie parallel with the long axis of the spine, especially in its neck, and had a preferential orientation in the long axis of the spine at the level of the synaptic junction. It was not always clear that filaments parallel with the plane of the section fell into the two size classes seen in fractured, etched tissue. However, when filaments were viewed in cross-section,

FIGURES 3–6 Fig. 3: Synapse between a parallel fiber and a Purkinje cell dendritic spine. The cross-fractured axoplasm of the parallel fiber bouton contains synaptic vesicles (short horizontal arrows) and its membrane has been fractured, revealing its cytoplasmic half. Only a portion of the spine membrane remains; its extracellular half lies in the hollow formed by the indentation into the parallel fiber bouton (in the cerebellum, the spines usually indent the presynaptic terminal). Scattered across the extracellular half of the fractured spine membrane (asterisk) is a collection of heterogeneous particles. At higher magnification, it is occasionally possible to find a contiguity between a particle on the spine fracture face and a fibril in the intercellular cleft between the spine and the parallel fiber axon (vertical arrow). × 160,000. Fig. 4: Etched cytoplasm in a Purkinje cell dendritic spine at a synaptic junction. The plane of fracture includes the cytoplasmic half of the plasma membrane of a parallel fiber (*Pre*). A fragment of the extracellular half of a spine membrane (asterisk) bears an aggregate of particles at the site of its junction with the parallel fiber axon. It is difficult to discern the exact demarcation between the fracture face and the true cytoplasmic surface of the spine membrane, but near the asterisk is an aggregate of particles arrayed on the extracellular half of the membrane, and to their left, in the cytoplasm of the etched spine just deep to the true cytoplasmic surface of the spine, there is a mesh of 4–6-nm filaments (upper arrow). A cluster of large particles, characteristic of the presynaptic aspect of the synaptic specialization (lower arrow) lies on the cytoplasmic half of the fractured axon membrane. × 130,000. Fig. 5: Stellate cell perikaryon at a synaptic junction with a parallel fiber. The extracellular half of the fractured plasmalemmal membrane is on the left of the illustration. A line of arrowheads at the top and bottom indicates the demarcation between the fracture face and the true inner surface revealed by etching, and two larger arrows pointing to the shelf of true inner surface of the membrane also demarcate an intervening region occupied by the synaptic junction. On the extracellular half of the fractured membrane is an array of somewhat heterogeneous particles characteristic of the postsynaptic aspects of synaptic junctions. In the etched cytoplasm co-extensive with the synaptic junction, there is a web of 4–6-nm filaments inserting on the true inner surface of the membrane, which obscures the true inner surface of the membrane. A 9–10-nm filament courses through the etched cytoplasm, deep to this web and slightly lateral to the site of the synaptic junction (oblique arrow). Granules of various sizes lie between and on these filaments. × 250,000. Fig. 6: Plasmalemma of the cell body of a stellate interneuron in the cerebellar cortex. To the left of the illustration is the extracellular half of the fractured cell membrane. A line of arrowheads indicates the demarcation between the fracture face and the true inner surface of the membrane that has been revealed by etching. The true cytoplasmic surface of the membrane, outside of regions which have postsynaptic specializations, is marked by particles of various sizes. In the cytoplasm, just deep to these particles, are filaments of at least two different diameters, coursing in parallel with the inner membrane surface. × 250,000.

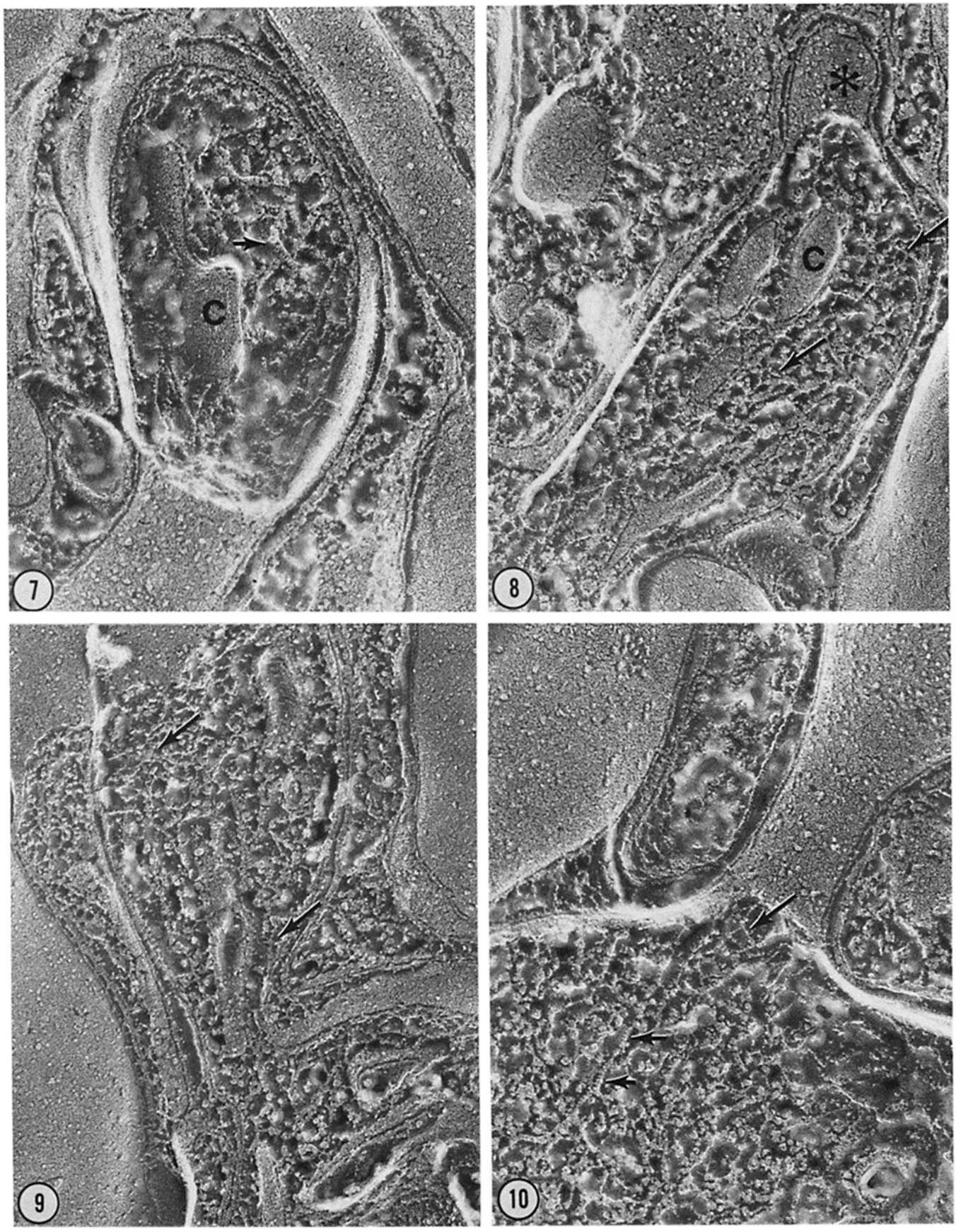
C
7
*
C
8
9
10

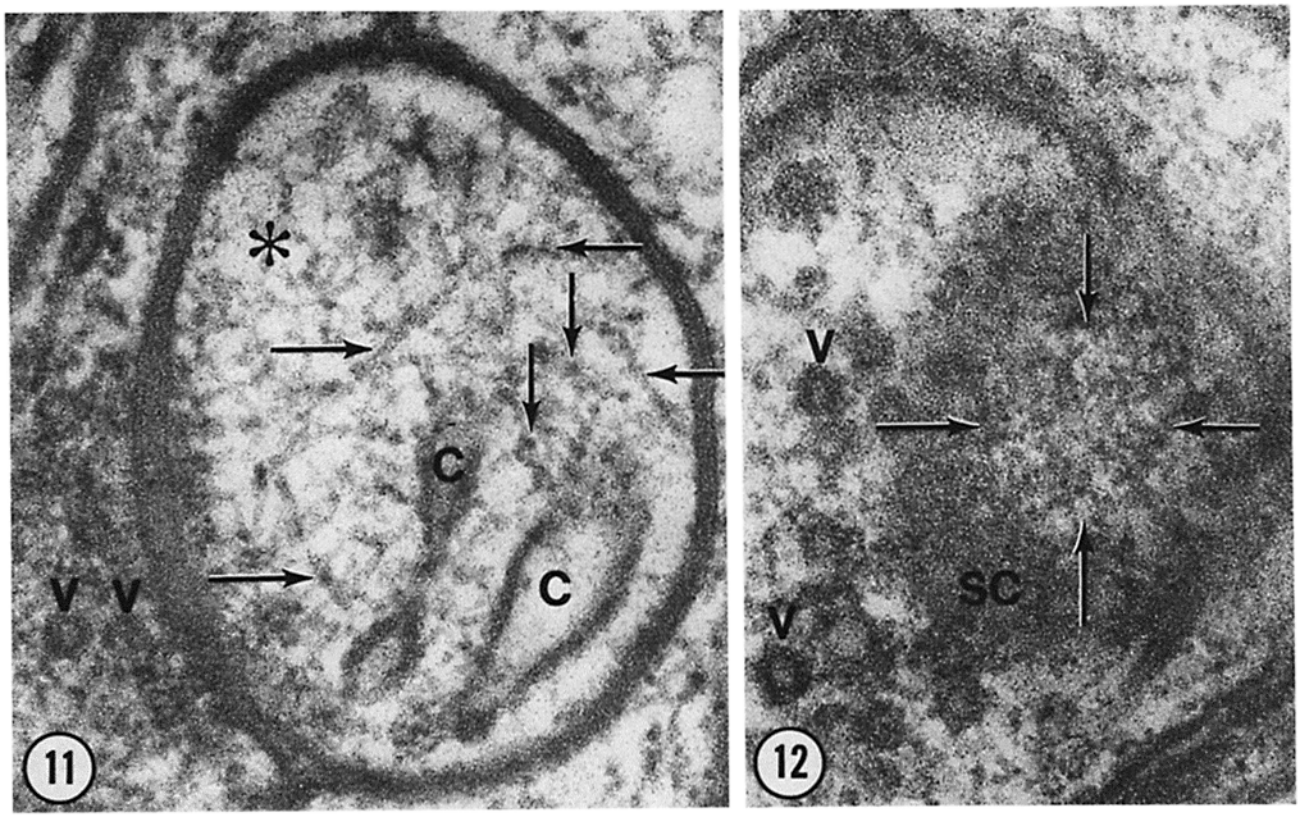


FIGURES 11 and 12 Fig. 11: Synaptic junction between a parallel fiber and a Purkinje cell spine, in rapidly frozen tissue fixed by freeze-substitution. Synaptic vesicles (*V*) are in the parallel fiber bouton, at the lower left. Surrounding the vesicles, in the diffusely electron-dense axoplasm at the presynaptic specialization, are several small annular profiles, which may represent cross-sectioned filaments encrusted with heavy metal stain. The postsynaptic electron-dense fuzz is co-extensive with the widened synaptic cleft, which in this preparation appears uniformly stained. In the cross-sectioned spine are membrane-bound cisterns (*C*) and many filaments, of at least two diameters. In the periphery of the spine, especially below the asterisk, are filaments of smaller diameter, which probably correspond to the 5–7-nm filaments in etched, replicated tissue. In the core of the spine are larger filaments, coursing in the plane of the section (horizontal arrows) or perpendicular to it (vertical arrows). These microfilaments probably correspond to the actin-like 9–10-nm filaments visualized in etched, replicated tissue. × 150,000. Fig. 12: Synaptic junction between a parallel fiber and a Purkinje cell spine, in oblique section. Synaptic vesicles (*V*) are in the presynaptic axoplasm, toward the left. The synaptic cleft (*SC*) appears as a broad zone of electron-dense material, without obvious substructure. The section has included a portion of the electron-dense fuzz of the postsynaptic specialization (ringed by arrows), in which individual filaments appear in cross-section as annular densities. These filaments correspond to the mesh of 4–6-nm filaments visualized in etched, replicated tissue (Fig. 5). × 160,000.

FIGURES 7–10 Fig. 7: Cytoplasmic structure in a cross-fractured dendritic spine. The cytoplasmic half of the fractured spine membrane is evident at the lower portion of the illustration. Etching of the cross-fractured spine cytoplasm has revealed a system of anastomotic and straight 5–7-nm filaments, some of which end close to the true cytoplasmic surface of the spine. Also, within the spine is the fractured membrane of a cistern (*C*). A few, larger filaments (arrowhead) are also present in the body of the spine. × 180,000. Fig. 8: Cross-fractured dendritic spine. The origin of the spine from the Purkinje dendrite is at the lower left. Large diameter filaments extend from the Purkinje dendrite into the base of the spine, and similar large diameter, 9–10-nm filaments are evident in the body of the spine. Also in the spine is a mesh of smaller (5–7 nm) filaments (arrows). The plane of fracture has also exposed the luminal half of several cisternal membranes (*C*). At the tip of the spine is an excrescence (asterisk); its membrane is marked by particles and filaments enter its neck. × 180,000. Fig. 9: Cross-fractured dendritic spine. The parent Purkinje dendrite is seen in cross fracture at the lower right. Within the body of the spine are several fractured cisterns. This spine also shows a complex mesh of 5–7-nm filaments (arrows). × 180,000. Fig. 10: Etched cytoplasm of a Purkinje dendrite at the origin of a Purkinje dendritic spine. The cytoplasmic half of the fractured spine membrane at the neck and at the proximal portion of the body of the spine is evident in the upper right. In the cross-fractured cytoplasm at the base of the spine there is a mesh of 5–7-nm filaments (oblique arrow). A larger diameter microfilament courses from the spine origin across the etched surface of the dendritic cytoplasm; this filament has a subtle periodicity (arrowheads) which is the basis for its tentative identification as an actin filament. The cluster of large particles on the cytoplasmic half of the fractured membrane of a parallel fiber axon (*upper left*) is probably a coated pit. × 180,000.

the two size classes were apparent (Fig. 11). The filaments constituting the electron-dense postsynaptic fuzz were quite discrete in freeze-substituted cerebellum (Fig. 12) and were slightly more electron-dense than the longer, fine filaments in the spine cytoplasm.

## DISCUSSION

Three distinct sets of filamentous elements were identified in Purkinje cell dendritic spines prepared by rapid-freezing and shallow-etching. A meshwork of short, straight filaments 4–6 nm in diameter extended up to 20 nm into the spine cytoplasm from the true cytoplasmic surface of the spine membrane at the synaptic junction; this mesh probably corresponds to the electron-dense fuzz seen in the thin-sectioned tissue prepared by conventional methods (20). There are also microfilaments 8–10 nm in diameter which share morphological characteristics with actin, and which are distributed principally in the body of the spine deep to the synaptic junction. The current preparative method also revealed a third set of filaments, 5–7 nm in diameter, concentrated in a zone 20–40-nm deep to the spine membrane and filling the neck and much of the body of the spine. Fig. 13 diagrams the distribution of these several types of filamentous elements.

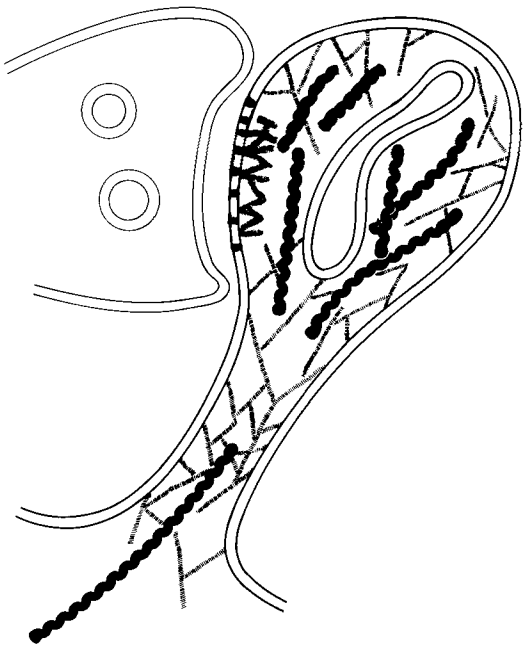

FIGURE 13 Diagram of filamentous elements in the cytoplasm of a Purkinje cell dendritic spine. A meshwork of short filaments 4–6 nm in diameter extends into the spine cytoplasm from the true inner surface of the spine membrane at the synaptic junction (these filaments as represented here are relatively larger than their actual diameter). The aggregate of particles associated with the extracellular half of the fractured membrane at the postsynaptic membrane is here represented as dark particles in the membrane. The exact relationship of the 4–6-nm filaments to the intramembrane particles is uncertain though some filaments may contact particles. A separate population of filaments 5–7 nm in diameter is concentrated near the spine membrane filling the neck and much of the body of the spine. These filaments end near the true inner surface of the membrane. A few 8–10-nm microfilaments are present in the body and neck of the spine; the representation here is intended to suggest that their periodicity in rotary-replicated preparations is due to the double helix of F-actin.

There is little reason to think that these filaments are an artifact of tissue preparation. Their distribution differs systematically and consistently in different cytoplasmic domains. They are present in freeze-substituted tissue and in fractured, etched tissue and therefore are unlikely to represent artifacts introduced after the instant of freezing. They are also clearly distinct from the concretions of cytoplasmic structure in deeper regions of tissue where ice crystals are larger. We restricted our attention to regions of the tissue where ice crystals were too small to recognize, presumably corresponding to regions in which freezing occurred in <2 ms (28, 43). It seems unlikely that nonfilamentous proteins somehow reorganized into filaments in this short interval. However, we cannot exclude the possibility that some structural changes occurred in the 25–35-s interval between decapitation and the instant of freezing.

In this study, cytoplasmic structure has been examined for the first time in synapses that have not been extracted, but have only been directly frozen and etched. Other workers have used detergents or other means to remove or dilute soluble cytoplasmic components to permit examination of insoluble components of nerves at high resolution after etching (20, 33). The drawback of such an approach, however, is that some structures are certainly lost, and others may be reorganized during the extraction or the etching. We have, instead, prevented granular cytoplasmic components from obscuring filamentous components of the cytoplasm by limiting the amount of etching to ~30 nm of water. The soluble cytoplasmic components that had been in this thin zone of ice now appear as irregular granules distributed rather uniformly over and among the filamentous structures revealed by the etching. At present few conclusions can be made about the nature of these granular structures, although it is likely that some are postsynaptic components such as calmodulin or other proteins characteristically associated with synaptic junctions (13).

The nature of the proteins constituting the various systems of filaments is also uncertain. It is probable that the anastomotic mesh at the synaptic junction corresponds to the postsynaptic density, seen in thin sections of extracted, separated synaptic fractions (2, 3, 5–7, 13, 34, 50, 56). The mesh probably represents the relatively insoluble, incompletely characterized "structural" component of the density. The larger, 8–10-nm filaments in fractured, etched spines have approximately the same diameter and longitudinal periodicity as filaments prepared by replication techniques and considered to be actin in other tissues (25, 32, 33). This identification would be consistent with biochemical analyses that detect actin in tissue fractions enriched with synaptic structures (5, 34; see also reference 21). Filaments thought to be actin also contact the filaments of the postsynaptic mesh at synaptic junctions between primary auditory afferents and the principal cells in the anteroventral cochlear nucleus (19, 20). There is little information about the composition of the fine 5–7-nm filaments. They resemble the "cross-linking wisps in the terminal web" illustrated by Hirokawa and Heuser (32) in a study of cytoskeletal organization in intestinal epithelial cells (eg., in Figs. 8 and 9). These authors suggest that the wisps in these cells may turn out to be monomers or oligomers of myosin.

The organization of the fine 5–7-nm filaments in Purkinje cell dendritic spines leads one to consider the possibility that they may have a role in the maintenance of spine shape.

These 5–7-nm filaments are concentrated in a zone 20–40-nm wide adjacent to the membrane of the spine, and they end in apposition to the true inner surface of the spine membrane everywhere except at the postsynaptic mesh. In particular, they fill the neck of the spine. If these filaments are attached to the spine membrane everywhere except at the postsynaptic mesh, they could provide the force that maintains the doubly inflected curve of the spine neck. Indeed, the manner in which spine shape is maintained has never been adequately explained. If the membranes of spines and dendrites do not have an intrinsic curvature, the spines should collapse into the dendrite unless structural support is provided. The fine filament system is in a position to provide this support.

The function of the actin-like microfilaments in the vicinity of synaptic junctions is not immediately apparent. They are preferentially distributed in parallel with the long axis of the spine, and are invariably found close to the postsynaptic mesh. In the portion of the spine body that funnels into the neck, these actin-like microfilaments course in parallel with the fine filaments and intersect them. Microfilaments also course close to the synaptic junctions on stellate cell perikarya and dendrites.

Do these microfilaments in the core of the Purkinje cell dendritic spines constitute a supporting skeleton contributing to a stable shape, or do they reflect a capacity to change shape? It has been proposed that changes in spine shape, especially in the diameter of the spine neck, would result in changes in the shape and amplitude of the synaptic current in the parent dendrite (45, 46). Several efforts have been made to correlate physiological plasticity of synaptic function (1, 54) with changes in spine shape (8, 39–41, 57). Recently, heavy meromyosin (11) and antibodies to actin (4) have been used to identify actin in hippocampal dendritic spines. Both groups of authors postulated that these actin-like filaments provided a basis for changes in spine shape.

Certain of the observations in the present study might be construed as evidence that Purkinje dendritic spines change shape. Smooth excrescences or bulges in these spines might represent the result of an abrupt decrease in spine volume occurring during the intense stimulation following decapitation and excision of the cerebellar slice. However, we are not aware of any physiological evidence that might indicate that dendritic spines of Purkinje cells undergo rapid changes in shape. Moreover, studies of the stereocilia of cochlear hair cells have shown that actin filaments there may serve to stabilize shape, and not be involved in movement or changes in shape (9, 10, 12, 55). For the present, the role of actin-like microfilaments in the vicinity of cerebellar synaptic junctions remains unknown.

The authors wish to thank Ms. D. Jackson and Ms. S. Cotter for their editorial assistance; Mr. L. Cherkas and Mr. N. Christakis are thanked for their assistance with the photography. Mr. William F. Graham has made major contributions to developing the freeze-fracture apparatus upon which this work depended.

This work was supported in part by NS 00353 (Teacher-Investigator Award to D. M. D. Landis) and NS 15573.

*Received for publication 13 January 1983, and in revised form 3 June 1983.*

## REFERENCES

1. Alger, B. E., and T. J. Teyler. 1976. Long-term and short-term plasticity in the CA1, CA3, and dentate gyrus regions of the rat hippocampal slice. *Brain Res.* 110:463–480.
2. Banker, G., L. Churchill, and C. W. Cotman. 1974. Proteins of the postsynaptic density. *J. Cell Biol.* 63:456–465.
3. Blomberg, F., R. S. Cohen, and P. Siekevitz. 1977. The structure of postsynaptic densities isolated from dog cerebral cortex. II. Characterization and arrangement of some of the major proteins within the structure. *J. Cell Biol.* 74:204–225.
4. Caceres, A., M. R. Payne, L. I. Binder, and O. Steward. 1983. Immunocytochemical localization of actin and microtubule-associated protein MAP2 in dendritic spines. *Proc. Natl. Acad. Sci. USA.* 80:1738–1742.
5. Carlin, R. K., D. J. Grab, R. S. Cohen, and P. Siekevitz. 1980. Isolation and characterization of postsynaptic densities from various brain regions: enrichment of different types of postsynaptic densities. *J. Cell Biol.* 86:831–843.
6. Cohen, R. S., F. Blomberg, K. Berzins, and P. Siekevitz. 1977. The structure of postsynaptic densities isolated from dog cerebral cortex. I. Overall morphology and protein composition. *J. Cell Biol.* 74:181–203.
7. Cotman, C. W., G. Banker, L. Churchill, and D. Taylor. 1974. Isolation of postsynaptic densities from rat brain. *J. Cell Biol.* 63:441–455.
8. Crick, F. 1982. Do dendritic spines twitch? *Trends Neurosci.* 5:44–46.
9. DeRosier, D. J., L. G. Tilney, and E. Egelman. 1980. Actin in the inner ear: the remarkable structure of the stereocilium. *Nature. (Lond.).* 287:291–296.
10. Dreckhahn, D., J. Kellner, H. G. Mannherz, U. Groschel-Stewart, J. Kendrick-Jones, and J. Scholey. 1982. Absence of myosin-like immunoreactivity in stereocilia of cochlear hair cells. *Nature. (Lond.).* 300:531–532.
11. Fifková, E., and R. J. Delay. 1982. Cytoplasmic actin in neuronal processes as a possible mediator of synaptic plasticity. *J. Cell Biol.* 95:345–350.
12. Flock, Å., and H. C. Cheung. 1977. Actin filaments in sensory hairs of inner ear receptor cells. *J. Cell Biol.* 75:339–343.
13. Grab, D. J., K. Berzins, R. S. Cohen, and P. Siekevitz. 1979. Presence of calmodulin in postsynaptic densities isolated from canine cerebral cortex. *J. Biol. Chem.* 254:8690–8696.
14. Gray, E. G. 1959. Axo-somatic and axo-dendritic synapses in the cerebral cortex: an electron microscopic study. *J. Anat. (Lond.).* 93:420–433.
15. Gray, E. G. 1982. Rehabilitating the dendritic spine. *Trends Neurosci.* 5:5–6.
16. Gray, E. G., and R. W. Guillery. 1966. Synaptic morphology in the normal and degenerating nervous system. *Int. Rev. Cytol.* 19:111–153.
17. Gross, H., E. Bas, and H. Moor. 1978. Freeze-fracturing in ultrahigh vacuum at −196°C. *J. Cell Biol.* 76:712–728.
18. Gross, H. 1979. Advances in ultrahigh vacuum freeze fracturing at very low specimen temperature. *In* Freeze Fracture: Methods, Artifacts, and Interpretations. J. E. Rash and C. S. Hudson, editors. Raven Press, New York. 127–139.
19. Gulley, R. L., D. M. D. Landis, and T. S. Reese. 1978. Internal organization of membranes and end-bulbs of Held in the anteroventral cochlear nucleus. *J. Comp. Neurol.* 180:707–742.
20. Gulley, R. L., and T. S. Reese. 1981. Cytoskeletal organization at the postsynaptic complex. *J. Cell Biol.* 91:298–302.
21. Hall, Z. W., B. W. Lubit, and J. H. Schwartz. 1981. Cytoplasmic actin in postsynaptic structures at the neuromuscular junction. *J. Cell Biol.* 90:789–792.
22. Hanna, R. B., A. Hirano, and G. D. Pappas. 1976. Membrane specializations of dendritic spines and glia in the weaver mouse cerebellum: a freeze-fracture study. *J. Cell Biol.* 68:403–410.
23. Hanna, R. B., T. S. Reese, R. L. Ornberg, D. C. Spray, and M. V. L. Bennett. 1981. Fresh frozen gap junctions: resolution of structural detail in the coupled and uncoupled states. *J. Cell Biol.* 91 (2, Pt. 2):125*a*. (Abstr.)
24. Hasty, D. L., and E. D. Hay. 1978. Freeze-fracture studies of the developing cell surface. II. Particle-free membrane blisters on glutaraldehyde-fixed corneal fibroblasts are artefacts. *J. Cell Biol.* 78:756–768.
25. Heuser, J. E., and M. W. Kirschner. 1980. Filament organization revealed in platinum replicas of freeze-dried cytoskeletons. *J. Cell Biol.* 86:212–234.
26. Heuser, J. E., T. S. Reese, and D. M. D. Landis. 1974. Functional changes in frog neuromuscular junctions studied with freeze-fracture. *J. Neurocytol.* 3:109–131.
27. Heuser, J. E., T. S. Reese, and D. M. D. Landis. 1976. Preservation of synaptic structure by rapid freezing. *Cold Spring Harbor Symp. Quant. Biol.* 40:17–24.
28. Heuser, J. E., T. S. Reese, M. J. Dennis, Y. Jan, L. Jan, and L. Evans. 1979. Synaptic vesicle exocytosis captured by quick freezing and correlated with quantal transmitter release. *J. Cell Biol.* 81:275–300.
29. Heuser, J. E., and T. S. Reese. 1981. Structural changes after transmitter release at the frog neuromuscular junction. *J. Cell Biol.* 88:564–580.
30. Heuser, J. E., and S. R. Salpeter. 1979. Organization of acetylcholine receptors in quick-frozen, deep-etched, and rotary-replicated *Torpedo* postsynaptic membrane. *J. Cell Biol.* 82:150–173.
31. Heuser, J. 1980. Three-dimensional visualization of coated vesicle formation in fibroblasts. *J. Cell Biol.* 84:560–583.
32. Hirokawa, N., and J. E. Heuser. 1981. Quick-freeze, deep-etch visualization of the cytoskeleton beneath surface differentiations of intestinal epithelial cells. *J. Cell Biol.* 91:399–409.
33. Hirokawa, N., and J. E. Heuser. 1982. Internal and external differentiations of the postsynaptic membrane at the neuromuscular junction. *J. Neurocytol.* 11:487–510.
34. Kelly, P. T., and C. W. Cotman. 1978. Synaptic proteins: characterization of tubulin and actin and identification of a distinct postsynaptic density polypeptide. *J. Cell Biol.* 79:173–183.
35. Kirchanski, S., A. Elgsaeter, and D. Branton. 1979. Low-temperature freeze fracturing to avoid plastic distortion. *In* Freeze Fracture: Methods, Artifacts, and Interpretations. J. E. Rash and C. S. Hudson, editors. Raven Press, New York. 149–152.
36. Landis, D. M. D., and T. S. Reese. 1974. Differences in membrane structure between excitatory and inhibitory synapses in the cerebellar cortex. *J. Comp. Neurol.* 155:93–126.
37. Landis, D. M. D., and T. S. Reese. 1977. Structure of the Purkinje cell membrane in staggerer and weaver mutant mice. *J. Comp. Neurol.* 171:247–260.
38. Landis, D. M. D., T. S. Reese, R. L. Ornberg, and W. F. Graham. 1981. Substructure in astrocytic assemblies demonstrated by rapid freezing and low-temperature freeze fracturing. *Proc. Soc. Neurosci.* 7:305.
39. Lee, K. S., F. Schottler, M. Oliver, and G. Lynch. 1980. Brief bursts of high-frequency stimulation produce two types of structural change in the rat hippocampus. *J. Neurophysiol. (Bethesda).* 44:247–258.
40. Moshkov, D. A., L. L. Petrovskaia, and A. G. Bragin. 1977. Post-tetanic changes in the ultrastructure of the giant spinal synapses in hippocampal field CA3. *Dokl. Akad. Nauk. SSSR.* 237:1525–1528.
41. Moshkov, D. A., L. L. Petrovskaia, and A. G. Bragin. 1980. Ultrastructural study of the bases of postsynaptic potentiation in hippocampal sections by the freeze-substitution method. *Tsitologiya.* 22:20–26.
42. Pappas, G. D., and D. P. Purpura. 1961. Fine structure of dendrites in the superficial

neocortical neuropil. *Exp. Neurol.* 4:507–530.
43. Ornberg, R. L., and T. S. Reese. 1979. Artifacts of freezing in Limulus amebocytes. *In* Freeze Fracture: Methods, Artifacts and Interpretations. J. E. Rash and C. S. Hudson, editors. Raven Press, New York. 89–97.
44. Pumplin, D. W., T. S. Reese, and R. Llinas. 1981. Are the presynaptic membrane particles the calcium channels? *Proc. Natl. Acad. Sci. USA.* 78:7210–7214.
45. Rall, W. 1970. Cable properties of dendrites and effects of synaptic location. *In* Excitatory Synaptic Mechanisms. Proceedings of the 5th International Meeting of Neurobiologists. P. Andersen and J. K. S. Jensen, editors. Universitetsforlaget, Oslo. 175–187.
46. Rall, W. 1974. Dendritic spines, synaptic potency and neuronal plasticity. *In* Cellular Mechanisms Subserving Changes in Neuronal Activity, C. Woody, K. Brown, T. Crow, and J. Knispel, editors. Brain Information Service, University of California Los Angeles.
47. Ramon y Cajal, S. 1891. Sur la structure de l'ecorce cerebrale de quelques mammiferes. *Cellule.* 7:124–176.
48. Ramon y Cajal, S. 1896. Les epines collaterales des cellules du cerveau colorees au bleu de methylene. *Rev. Trim. Microgr.* 1:5–19.
49. Rash, J. E., and M. H. Ellisman. 1974. Studies of excitable membranes. I. Macromolecular specializations of the neuromuscular junction and the nonjunctional sarcolemma. *J. Cell Biol.* 63:567–586.
50. Sampedro, M. N., C. M. Bussineau, and C. W. Cotman. 1981. Postsynaptic density antigens: preparation and characterization of an antiserum against postsynaptic densities. *J. Cell Biol.* 90:675–686.
51. Schnapp, B. J., and Reese, T. S. 1982. Cytoplasmic structure in rapid-frozen axons. *J. Cell Biol.* 94:667–679.
52. Sleytr, U. B., and A. W. Robards. 1977. Plastic deformation during freeze-cleavage: a review. *J. Microsc.* 110:1–25.
53. Swindale, N. V. 1981. Dendritic spines only connect. *Trends Neurosci.* 4:240–241.
54. Teyler, T. J. 1976. Plasticity in the hippocampus: a model systems approach. *Adv. Psychobiol.* 3:301–326.
55. Tilney, L. G., D. J. DeRosier, and M. J. Mulroy. 1980. The organization of actin filaments in the stereocilia of cochlear hair cells. *J. Cell Biol.* 86:244–259.
56. Ueda, T., P. Greengard, K. Berzins, R. S. Cohen, F. Blomberg, D. J. Grab, and P. Siekevitz. 1979. Subcellular distribution in cerebral cortex of two proteins phosphorylated by a cAMP-dependent protein kinase. *J. Cell Biol.* 83:308–319.
57. Van Harreveld, A., and E. Fifkova. 1975. Swelling of dendritic spines in the fascia dentata after stimulation of the perforant fibers as a mechanism of post-tetanic potentiation. *Exp. Neurol.* 49:736–749.
58. Van Harreveld, A., and J. Crowell. 1964. Electron microscopy after rapid freezing on a metal surface and substitution fixation. *Anat. Rec.* 149:381–386.
59. Van Harreveld, A., J. Crowell, and S. K. Malhotra. 1965. A study of extracellular space in central nervous tissue by freeze-substitution. *J. Cell Biol.* 25:117–137.